

the data given in Table I, there seems to be no general relation between R_e and a power of ρ . For each of the four pseudonickels, however, the points corresponding to the three temperatures do fall on straight lines not passing through the origin, when R_e is plotted against ρ^2 . Pure Fe and Fe alloyed with some low percentages of Si obey the relation¹⁷ $R_1 = A\rho^{1.9}$. However, there is a deviation from the simple power law at low resistivities which so often occurs.

The treatment of R_e given by Luttinger,¹⁰ based on the theory of electrical transport phenomena of Kohn and Luttinger,¹⁸ gives in addition to a ρ^2 dependence, a linear term in ρ . This theory, which is applicable only to impurity limited resistivity, suggests fitting the data for the 4 samples for a single low temperature

¹⁷ C. Kooi, Phys. Rev. **95**, 843 (1954).

¹⁸ W. Kohn and J. M. Luttinger, Phys. Rev. **108**, 590 (1957).

with an equation of the form

$$R_e = a + b\rho + c\rho^2.$$

We were unsuccessful in this, as were Dreesen and Pugh¹⁴ and Beitel and Pugh¹⁶ in investigating Ni-Pd and Fe-Co alloys respectively. This is not too surprising in view of the highly simplified model for which the calculations have been carried through.

ACKNOWLEDGMENTS

We wish to thank the various members of the Department of Physics at the Carnegie Institute of Technology who have contributed helpful advice and discussion, particularly Dr. J. A. Dreesen. We are also grateful to the Westinghouse Electric Corporation for furnishing sample materials.

Energy Transfer within a Spin System*

D. F. HOLCOMB, B. PEDERSEN,[†] AND T. R. SLIKER

Laboratory of Atomic and Solid-State Physics, Cornell University, Ithaca, New York

(Received May 2, 1961)

The nature of the transfer, within a single nuclear spin system, of energy absorbed from an external source of radio-frequency magnetic field has been investigated by a double-irradiation technique. Energy from a high-power oscillator running at fixed frequency is absorbed by the nuclear spin system. The frequency of a second, low-level oscillator is then swept through the nuclear resonance, sampling the line shape existing in the presence of the strong rf field from the fixed-frequency oscillator. Particular spin systems investigated were the proton system in single crystalline $\text{CaSO}_4 \cdot 2\text{H}_2\text{O}$, and the Al^{27} system in aluminum metal. In alumi-

num, the technique gives direct experimental verification of a completely homogeneous saturation behavior, a behavior expected from elementary considerations. It also gives further verification of the Redfield saturation theory. In $\text{CaSO}_4 \cdot 2\text{H}_2\text{O}$, an enhancement effect is observed which allows one to determine the importance of double-flip spin-lattice relaxation processes. The technique could be usefully applied to many spin systems to determine the degree of inhomogeneity in the resonance line broadening.

IN interpreting results of spin resonance experiments, one is often interested in the nature and efficiency of processes by which energy absorbed by part of the spin system from an applied rf magnetic field is shared with the rest of the spin system. The problem is only of interest, of course, when the spectral distribution function of the resonance line, $g(\omega)$, is determined by some mechanism other than lifetime broadening. Knowledge of the nature and efficiency of the energy transfer is crucial in interpreting the results of steady-power magnetic resonance saturation experiments. As a matter of fact, it is often uncertainties about the behavior of this energy transfer which make saturation determinations of T_1 , the spin-lattice relaxation time, inferior to direct transient measurements of T_1 .

We have applied a double-resonance technique to determine experimentally some facets of the behavior of this energy transfer.¹ Two representative nuclear spin systems have been investigated. One is the proton system in $\text{CaSO}_4 \cdot 2\text{H}_2\text{O}$ and the other the Al^{27} system in aluminum metal. The sample is subjected to a fixed-frequency saturating rf magnetic field of amplitude $2H_1$, at frequency ω_1 . ω_1 is set at some appropriate position within the frequency spread of the resonance line. We deal entirely with cases in which H_1 is less than the resonance linewidth. Then the frequency of a second, low-level oscillator is swept through the region of the resonance line, and the line shape in the presence of H_1 is measured by this second, tickler oscillator. Details of the experimental arrangement are described in the next section. As a result of this sampling with the second oscillator, we determine the manner in

* Supported in part by the U. S. Office of Naval Research and in part by a grant from the Alfred P. Sloan Foundation to one of the authors (DFH).

[†] Permanent address: Central Institute for Industrial Research, Oslo, Norway.

¹ Similar double-resonance experiments have been performed by W. A. Anderson, Phys. Rev. **102**, 151 (1956) and by J. Itoh and R. Kusaka, J. Phys. Soc. Japan **14**, 492 (1959).

which rf power pumped into the spin system at ω_1 is distributed among spins in other parts of the spectral distribution.

I. EXPERIMENTAL DETAILS

The experiments were done at a resonant frequency of 12.4 Mc/sec for protons in $\text{CaSO}_4 \cdot 2\text{H}_2\text{O}$ (gypsum) and at 6.6 Mc/sec for Al^{27} . The standard crossed-coil probe from a Varian 4200B spectrometer was used, with the Varian transmitter providing the saturating H_1 (up to about 1.0 gauss). For the proton work, the receiver coil in the probe served as the tank coil for a Pound-Knight² marginal oscillator, which was thus used to inspect the resonance absorption in the presence of the large H_1 provided by the Varian transmitter. For the aluminum measurements, because of lower signal strength, a separate receiver coil for the Pound-Knight oscillator was inserted into the probe. The frequency of the sampling oscillator was swept through the resonance with a motor-driven capacitor while the frequency of H_1 remained fixed. The rf magnetic field in the sample from the sampling oscillator was well below the saturation level, so that this oscillator did not appreciably disturb the spin system. H_0 was modulated at a frequency of 210 cps.

The chief experimental problem in this arrangement is the exclusion of signal from the saturating oscillator picked up in the receiver coil of the sampling oscillator, since the oscillators were operated at frequencies differing by as little as 2 kc/sec. There are really two spurious signals which concern one. The first is the direct signal from the Varian transmitter coil. The second is the nuclear induction signal excited by the Varian transmitter—we want to observe with the sampling oscillator only the nuclear signal excited by its own rf field. The direct signal can be largely eliminated using the standard balancing adjustments in the Varian probe. This adjustment is conveniently made by tuning the oscillators very closely together, then observing the beat signal from the audio section of the sampling oscillator. The paddles in the Varian probe are then adjusted to reduce this beat signal to zero. To eliminate any residual direct signal plus the nuclear signal excited by the Varian oscillator it is necessary to employ proper frequency filtering in the detecting system of the Pound circuit. The elimination is made possible by the fact that the rf voltage in the tank coil of the sampling oscillator, at frequency ω_2 , is very much larger than the pickup voltage at the Varian frequency ω_1 . The sum of the signals at ω_2 and ω_1 , after rf amplification, is fed to the detector. Since the signal at ω_1 is small relative to the carrier at ω_2 , after detection we have audio signals at $\omega_2 - \omega_1$ and $\omega_2 + \omega_1 \pm \omega_m$ resulting from the presence of ω_1 , but a dc component determined entirely by the ω_2 carrier amplitude. It is necessary that the detector time constant be short

enough that these difference frequency signals be undistorted. In our experiments, $RC = 1 \mu\text{sec}$ for the detector. Thus, after the detector, we have a rectified signal with a small modulation at the difference frequency and its sidebands, in addition to the modulation by the desired nuclear signal at frequency ω_m . We then filter the audio signal with a twin-T network followed by phase-sensitive detector tuned to frequency ω_m . Thus, the desired nuclear signal at ω_m is passed, but the unwanted signals at frequencies much higher than ω_m are highly attenuated. The minimum value of $\omega_2 - \omega_1$ at which the sampling oscillator performs satisfactorily is ultimately limited by pulling of the frequency of the sampling oscillator by the Varian oscillator. The minimum value of $f_2 - f_1$ for satisfactory operation was about 2 kc/sec.

The narrow-banding was done using modulation of H_0 , the external magnetic field. Actually, frequency modulation of the sampling oscillator would be better for these experiments, since modulating H_0 has the effect of sweeping H_1 through a swath of resonance linewidth equal to twice the field modulation amplitude. Thus, if H_1 is of saturating strength, the dependence of M_z , the component of nuclear magnetization parallel to H_0 , on the position of ω_1 may introduce distortion into the line shape observed by the sampling oscillator. Redfield³ discusses modulation effects of the type we have, with $\omega_m > 1/T_1$. A number of our experiments were performed with ω_1 located on the peak of the resonance line. In this case, there is no contribution at the phase-sensitive detection frequency ω_m from the undesired modulation effects. Several experiments in aluminum were performed with ω_1 off resonance. Influence of modulation of the position of ω_1 on the resonance curve in these experiments is discussed in Sec. III.

II. EXPERIMENTS IN $\text{CaSO}_4 \cdot 2\text{H}_2\text{O}$

The normal single-resonance absorption derivative of the proton line, for the crystal orientation used, is

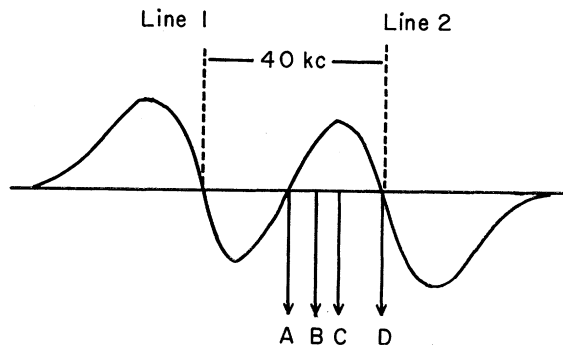


FIG. 1. Sketch of proton resonance absorption derivative in $\text{CaSO}_4 \cdot 2\text{H}_2\text{O}$, illustrating double-resonance experiment. The frequency of the saturating oscillator, ω_1 , is located at one of the positions A, B, C, or D. The frequency of the sampling oscillator is then swept through the resonance.

² R. V. Pound and W. D. Knight, Rev. Sci. Instr. **21**, 219 (1950).

³ A. G. Redfield, Phys. Rev. **98**, 1787 (1955).

sketched in Fig. 1. ($H_1 \approx 0$.) The crystal was oriented with H_0 parallel to the b axis. All H-H pairs in various H_2O molecules are then magnetically equivalent, the H-H vector making an angle of 38.5° with the b axis. Hence, one sees a two-peak spectrum with a peak-peak separation of 9.5 gauss.⁴ Double-irradiation experiments were performed with the frequency ω_1 at positions A , B , C , and D in the pattern, at various H_1 levels. In each case, the frequency ω_2 was then swept through the whole pattern, and the resonance derivative signal at frequency ω_2 recorded.

One obvious but important point should be emphasized. The changes in linewidth and line shape observed for dipolar-broadened lines in a conventional magnetic resonance experiment as H_1 is raised into the saturation region arise primarily from the direct effect of H_1 on the part of the resonance line which lies within a frequency width γH_1 of the oscillator frequency ω_1 . Any changes in width or shape observed in the double-resonance experiment would arise from fundamental

TABLE I. Resonance enhancement in $\text{CaSO}_4 \cdot 2\text{H}_2\text{O}$. For these measurements, ω_1 is located at position D on line 2 (see Fig. 1).

| H_1 (gauss) | Relative amplitude of line 1 (Error ± 0.05 on all) |
|---------------|---|
| 0.0011 | 1.00 |
| 0.0034 | 1.06 |
| 0.0071 | 1.12 |
| 0.013 | 1.22 |
| 0.030 | 1.37 |
| 0.055 | 1.44 |
| 0.093 | 1.37 |
| 0.16 | 1.37 |
| 0.24 | 1.37 |

changes in the line-shape function induced by the saturating rf field, since we observe with the sampling oscillator not the part of the spin system directly affected by H_1 , but the rest of the spectral distribution. Most of the spectral distribution of spins feels the saturating H_1 only indirectly, through the spin-spin interactions, provided, of course, $H_1 \ll \text{linewidth}$.

The most important experimental results concerning the line shape and width can be summarized rather briefly.

(1) The 40 kc/sec separation of the main peaks (which agrees with Pake's⁴ measurements) was unchanged throughout the range of H_1 used, for all positions of ω_1 . Changes in the peak positions occur as H_1 becomes appreciable compared to the peak separation (9.5 gauss), as shown by the work of Itoh and Kusaka¹ on a similar system.

(2) The peak-to-peak derivative width of line 1 remained unchanged throughout the experiments.

(3) The peak-to-peak derivative width of line 2 remained unchanged with ω_1 at position A , the center

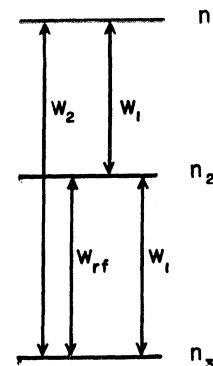


FIG. 2. Energy levels of two-spin system. n_1 , n_2 , and n_3 are the populations in the three levels. w_1 and w_2 are the spin-lattice transition probabilities between the levels indicated. w_{rf} is the transition probability for transitions induced by H_1 .

of the pattern, or at position D , on the peak of line 2. However, with ω_1 at positions B or C , the peak-to-peak derivative width was observed to decrease from its unsaturated value of 16 kc/sec to 12 kc/sec at maximum H_1 , 0.24 gauss. Discussion of this result will be deferred until discussion of a similar result in aluminum.

An interesting experimental result involving changes in line intensity was obtained with ω_1 at position D , i.e., at the center of one peak. In this case, the resonance signal observed from line 1 increased in size as H_1 was increased into the saturation region. It should be remembered that the sampling circuit is run at a constant, nonsaturating rf level, so that the signal strength is a direct measure of the population difference for the two levels involved in the line 1 transition. (The enhancement effect was also observed, to a lesser degree, with the frequency ω_1 at positions C and B , Fig. 1.) The amplitude of the signal from the sampling oscillator for line 1 is given as a function of H_1 from the saturating oscillator in Table I, for the case of ω_1 at position D .

The enhancement effect can be understood if we consider the proton spin system as a system of isolated proton pairs, following Pake.⁴ For the crystal orientation we have used, the interproton vectors of all pairs make the same angle with H_0 . In such a case, we describe the system by means of a three-level energy diagram. See Fig. 2. We have omitted the singlet level, since, for the isolated pairs, there are no transitions from singlet to triplet levels. (In actuality, the singlet levels of the pairs play an important role in relaxation processes in the crystals.⁵ For purposes of the present discussion, we can ignore the singlet level.) Certain relaxation processes in such a two-proton system have been discussed by Bloembergen.⁶ He discusses just the experimental situation we have here. We saturate heavily the lower transition in Fig. 2. That is, $n_3 - n_2$ is driven to zero. We observe the population difference between the upper two levels. Bloembergen shows, using the Bloch⁷ formalism, that we may expect to

⁵ D. F. Holcomb and B. Pedersen, *Bull. Am. Phys. Soc.* **6**, 103 (1961).

⁶ N. Bloembergen, *Phys. Rev.* **104**, 1542 (1956).

⁷ F. Bloch, *Phys. Rev.* **102**, 104 (1956).

⁴ G. E. Pake, *J. Chem. Phys.* **16**, 327 (1948).

find $n_2 - n_1$ enhanced over its thermal equilibrium value by the factor

$$\frac{n_2 - n_1}{(n_2 - n_1)_{\text{eq}}} = \frac{w_1 + 2w_2}{w_1 + w_2}, \quad (1)$$

where w_1 is the probability for $\Delta m = \pm 1$ transitions induced by the spin-lattice interaction, and w_2 is the transition probability for $\Delta m = \pm 2$. The result given above as Eq. (1) can also be straightforwardly obtained by writing down the rate equations for dn_1/dt , dn_2/dt , and dn_3/dt , including the effects of w_1 , w_2 , and w_{rf} , and solving for the dynamic equilibrium value of $n_2 - n_1$ with the condition $w_{\text{rf}} \gg w_1, w_2$.

Because of the fact that our system, in reality, consists of rather broad energy levels, and the two transitions indicated in Fig. 2 are not perfectly resolved, we would not expect the gypsum system to be described by Eq. (1) at very high rf levels. There will be some saturation of the upper transition because of spin-spin interactions. In Table I, there is some indication that our signal amplitude is beginning to fall at the highest attainable values of H_1 . The level of H_1 at which this saturation effect begins can be shown to be reasonable on the basis of the observed line shape and the value of the spin-lattice relaxation time, T_1 , which is 0.4 sec at room temperature. Interpretation of data of Table I in the light of Eq. (1) indicates a ratio w_2/w_1 of about $\frac{1}{2}$. This result was initially very surprising to us, since we assumed that the relaxation mechanism involved paramagnetic impurities and a spin diffusion process, in which case the w_2 transition probability might be expected to be small. (A simultaneous double flip of one pair of nuclei against another in the spin diffusion process has a very low transition probability; it involves a second-order matrix element.) The experimental value for w_2/w_1 led us to investigate the relaxation mechanism for the protons in $\text{CaSO}_4 \cdot 2\text{H}_2\text{O}$.⁵ The relaxation mechanism arises from the inter-pair nuclear dipole-dipole interaction, modulated by a 180° reorientation of the water molecules, and the w_2/w_1 ratio should indeed be appreciable.

III. ALUMINUM

A set of double-irradiation experiments was also performed on the Al^{27} spin system in aluminum metal. The sample consisted of a finely divided 99.9% pure aluminum powder.⁸ The characteristics of the Al^{27} resonance have been extensively investigated.^{3,9,10} The linewidth arises from direct dipole-dipole interaction between nuclei, plus, apparently, a small contribution from an electron-coupled dipole-dipole interaction.³

⁸ We are indebted to J. A. Nock of the Aluminum Company of America Research Laboratories for supplying the aluminum samples.

⁹ H. S. Gutowsky and B. R. McGarvey, J. Chem. Phys. **20**, 1472 (1952).

¹⁰ J. J. Spokas and C. P. Slichter, Phys. Rev. **113**, 1462 (1959).

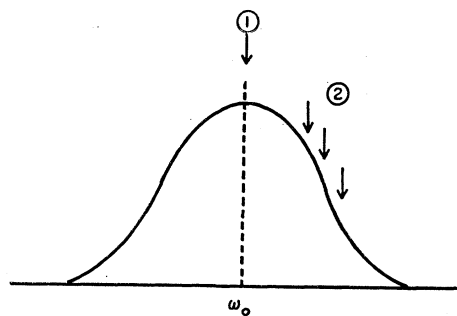


FIG. 3. Sketch illustrating double-resonance experiment in aluminum. ω_1 is located either at resonance, position 1, or at one of the positions 2.

Figure 3 indicates the experiments we have performed in aluminum. The frequency ω_1 was set either at resonance, position 1, or at various positions 2 in the wing of the line. The frequency of the sampling oscillator was then swept through the line, and the line shape and amplitude as given by the sampling oscillator was measured as a function of the magnitude of H_1 .

H_1 was measured roughly with a pickup coil located at the position of the sample. Values of the saturation factor S [$S = \frac{1}{2}\gamma^2 H_1^2 T_1 g(\nu_0)$] were determined more precisely, however, by observing the single resonance saturation behavior of the peak of the Al resonance line, with the sample in position for the double-irradiation experiments. The saturation behavior of χ'' at resonance is the same in all theories of saturation, and is given by the relation

$$\chi_{\text{res}}'' \propto 1/(1+S). \quad (2)$$

A fit of the data of χ_{res}'' as a function of V_{rf}^2 , where V_{rf} is the rf voltage observed across the transmitter coil, to Eq. (2) allows a determination of S as a function of V_{rf} . As a cross check on this determination, the values of S so obtained were combined with Redfield's T_1 measurement¹¹ and $g(\nu_0)$ to give a scale of H_1 vs V_{rf} . Measurements of the saturational line narrowing of the single resonance line as a function of V_{rf} were then made and fitted to Redfield's data on the same phenomenon.¹² (Redfield's values of H_1 were obtained from his rotary saturation scheme.³) Values of H_1 obtained by fitting the line-narrowing data agreed within 10% with those obtained from the saturation measurements.

ω_1 at Resonance

With ω_1 at resonance, the line shape, as detected by the sampling oscillator, was unchanged throughout the range of H_1 available. (Maximum H_1 gave a saturation factor S of approximately 10.) This result is not surprising, but does confirm directly the picture of such a spin system as having a completely homogeneous

¹¹ A. G. Redfield, Phys. Rev. **101**, 67 (1956).

¹² D. F. Holcomb, Phys. Rev. **112**, 1599 (1958).

saturation behavior. The Redfield saturation theory³ does not modify this picture, for the case of ω_1 at resonance, and with $H_1 \ll \text{linewidth}$.

The integrated area of the sampling oscillator absorption curve is essentially a measurement of M_z , the component of nuclear magnetization in the direction of H_0 . For the case of ω_1 at resonance, the line shape is independent of the magnitude of H_1 , and we can simply use the peak derivative signal from the sampling oscillator as a measure of the relative size of M_z . The experimental variation of M_z with H_1 is given by the relation

$$M_z = M_0 / (1 + S). \quad (3)$$

Equation (3) is the variation of M_z with H_1 given by the Bloch equations¹³ for the case of H_1 at resonance. It should be noted that if one modifies the Bloch equations, as suggested by Redfield,³ by inserting a different transverse relaxation time for decay along the direction of H_1 in the frame rotating at ω_1 , the steady-state solution for M_z is given by the relation

$$M_z = M_0 \frac{1 + (\omega_1 - \omega_0)^2 T_2 T_{2e}}{1 + (\omega_1 - \omega_0)^2 T_2 T_{2e} + \gamma^2 H_1^2 T_1 T_2}, \quad (4)$$

where T_2 is the transverse decay time in a direction perpendicular to the direction of H_1 in the rotating frame, and T_{2e} is the transverse decay time parallel to the direction of H_1 . At resonance, we see that the replacement of T_2 by T_{2e} for the decay parallel to H_1 does not affect the expression for M_z . The experimental result (3) is thus also described correctly by the modified Bloch equations. (See Appendix for further discussion of these modified equations.)

M_z with ω_1 off Resonance

With ω_1 off resonance, the sampling oscillator derivative curve must be integrated twice to find M_z , since the shape changes with H_1 level. (See next section.) We have not made a complete set of measurements of M_z with ω_1 off resonance, because of some difficulty with small frequency drifts of the Varian oscillator at high power levels. These drifts are serious, because of the sharp dependence of M_z on the frequency difference $\omega_1 - \omega_2$. In all our experiments, ω_1 was far enough off resonance so that the effective static field, H_{er} , in a coordinate system rotating at frequency ω_1 was determined primarily by $(H_0 - \omega_1/\gamma)$ rather than by H_1 . Measurements that we have made agree with the expression for $M_{z\rho}$ as a function of H_{er} derived by Redfield [Eq. (38) in reference 3]. In particular, it is clear that once H_1 is well into the saturation region, there is no further major decrease of M_z with increasing H_1 . We will not elaborate further on these measurements, since a much more careful and complete set of

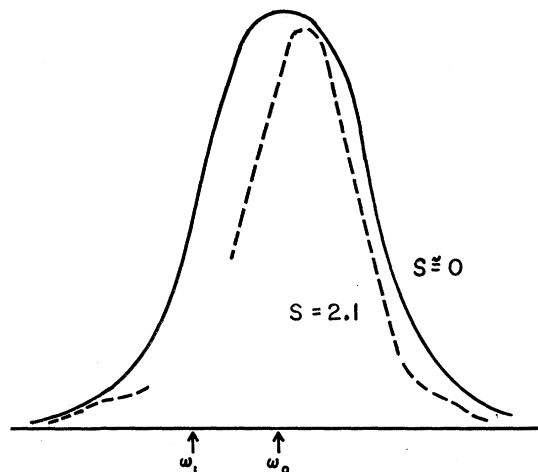


FIG. 4. Line shape observed by tickler oscillator for two values of the saturation parameter S . The amplitude of the curve for $S=2.1$ has been multiplied by 2 for ease in comparing the shapes of the two curves. The gap in the dashed curve shows the region which is unobservable because of interaction between the two oscillators.

similar measurements has been made by Goldburg¹⁴ in NaCl, by a somewhat different technique.

Line Shape with ω_1 off Resonance

When ω_1 is off resonance, the line shape, as detected by the sampling oscillator, changes as H_1 is raised into the region of heavy saturation. Figure 4 shows the integrated derivative curve for two cases, $S \approx 0$ and $S = 2.1$. The shape does not change significantly for saturation levels above $S = 2.1$, up to our maximum attainable value, $S = 10$. The simple assumption has often been made for a homogeneously broadened line such as that in aluminum that the spin-spin interactions maintain the line-shape function $g(\omega)$ unchanged until H_1 becomes of the order of the linewidth. (It should be mentioned that this assumption is not an integral part of the Bloembergen, Purcell, and Pound saturation theory,¹⁵ since they recognized the possibility that $g(\omega)$ might change.) It is clear that $g(\omega)$ does change somewhat, the line being narrowed and the peak displaced off resonance. It will be remembered that the same narrowing phenomenon was observed in gypsum when ω_1 and ω_2 were both in the same half of the line. Redfield's description of the spin system in terms of a well-defined effective spin temperature in the rotating frame makes such a result understandable. Before discussing Fig. 4 in terms of the Redfield picture, one should point out that there is a possible slight distortion of the true line shape as a result of our experimental technique. The source of this distortion was mentioned in Sec. I. Because we are modulating H_0 (amplitude

¹⁴ W. I. Goldburg, Phys. Rev. **122**, 831 (1961).

¹⁵ N. Bloembergen, E. M. Purcell, and R. V. Pound, Phys. Rev. **73**, 679 (1948).

¹³ F. Bloch, Phys. Rev. **70**, 460 (1946).

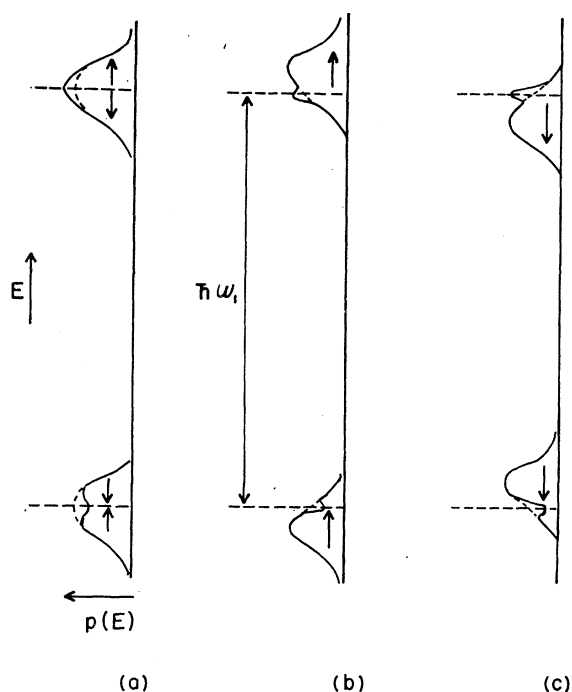


FIG. 5. Diagram illustrating the effects of spin-spin relaxation processes for various positions of ω_1 relative to ω_0 . $p(E)$, the population of energy levels, as observed in the magnetic resonance experiment, is plotted as a function of the energy. The arrows in each case indicate the net effect of the spin-spin processes in transferring spins within the local field energy spread.

$H_m = 1.0$ gauss) rather than ω_2 , the position of H_1 with respect to resonance center is also modulated. The resulting modulation of M_{zp} , the component of nuclear magnetization in the direction of the effective field, is very small, because of the fact that $\omega_m = 1320 \text{ sec}^{-1}$ and $1/T_1 = 180 \text{ sec}^{-1}$. The fast modulation means that M_{zp} remains essentially at the value corresponding to the midpoint of the modulation. However, there is still a fluctuating component in M_z at frequency ω_m , because the angle between the effective field, \mathbf{H}_{er} , and the external field, \mathbf{H}_0 , is being modulated. Any spurious contribution from this effect will alter the sampling oscillator derivative curve in two ways. (1) The zero of the derivative will shift toward the position of ω_1 . Note that this is the opposite direction to the shift observed in Fig. 4. (2) The derivative curve will be distorted so that its integral will not have the same base line at the two extremes of the resonance region. Since neither effect appears experimentally, we conclude that, at least qualitatively, the shape changes observed in Fig. 4 are real. We only discuss the line shape qualitatively, but we should point out that frequency modulation of ω_2 is necessary in order to observe absolutely no distortion of the line shape.

The line-shape measurements point out one intrinsic difference between our experiment and Goldburg's. We sample $g(\omega)$ in the presence of the saturating H_1 . He observes the free induction decay after an rf pulse.

This pulse follows the end of a saturating pulse with a time delay long compared to T_2 . Hence, the Fourier transform of the free induction decay gives the line shape appropriate to the case $H_1 = 0$.

It can be recognized on fairly simple grounds that a line-shape change such as that shown in Fig. 4 should not offend one. Figure 5 illustrates the sort of qualitative argument that can be used. The diagrams indicate population of energy levels, $p(E)$, as a function of energy as observed in the magnetic resonance experiment. (One understands, of course, that this does not represent a complete energy-level diagram of the spin system.) We view the saturation of a homogeneously broadened line as an imaginary two-step process.

Step 1. Energy absorption from the rf field corresponds to creation of a bulge in the upper energy-level population and a hole in the lower level population, as indicated in Fig. 5.

Step 2. This absorbed energy is dissipated throughout the energy-level distribution by the spin-spin relaxation processes. Figure 5(a) corresponds to the case of ω_1 at resonance. The mutual spin-flip processes are indicated schematically by the arrows. These processes involve no net energy input into the local field energy. That is, there need be no net change in the preferential alignment of nuclear moments in the magnetic fields of their neighbors. Figure 5(b) and (c) correspond to ω_1 off resonance, with $\omega_1 < \omega_0$ and $\omega_1 > \omega_0$, respectively. We have secured these situations by changing H_0 and leaving ω_1 constant. The arrows indicate the net effect of the spin-spin processes. In order to reestablish the dynamic equilibrium shape of the energy-level distribution, we require a net energy flow either into the local field energy [case (b)], or out of the local field energy [case (c)]. We should not be surprised if the establishment of the dynamic equilibrium leads to a different distribution of local field state population with ω_1 located off resonance. In particular, any inhibition of the effectiveness of T_2 processes by the necessity of appreciable energy exchange in cases (b) or (c) would lead to the line shape shown in Fig. 5. That is, the population difference for nuclei whose frequency is near ω_1 is smaller than for the nuclei on the other side of the resonance line.

Let us now, with Redfield, view the system in a frame rotating at ω_1 , and discuss the situation in terms of the distribution of effective energy in the rotating frame. At the different positions of ω_1 with respect to ω_0 , we have different distributions of the total effective energy between the effective external energy (the interaction energy of the spin system with \mathbf{H}_{er}) and the effective internal energy (the energy associated with preferential alignment of nuclei in the magnetic fields of their neighbors). If we describe the system in terms of an effective spin temperature in the rotating frame, this spin temperature would be different for different positions of H_1 . Consequently, we expect a different population distribution in the energy levels of the

transformed Hamiltonian. As we have mentioned above, the line shape has little further change with increasing H_1 once we are well into the saturation region. According to the Redfield picture, once we have arrived at a value of H_1 large enough to give sufficiently heavy saturation that the energy leak to the lattice by means of the T_1 processes is small, then both M_z and the line shape will be determined by the manner in which the energy-level populations, viewed in the rotating frame, arrange themselves into a canonical distribution. The magnitude of \mathbf{H}_{er} and the location of ω_1 with respect to resonance center will be the variables determining M_z and the line shape. In our experiments we have located ω_1 sufficiently far off resonance that \mathbf{H}_{er} is determined primarily by $(H_0 - \omega_1/\gamma)$. As H_1 becomes large enough to be a major factor in determining the magnitude of \mathbf{H}_{er} , then we would expect a more significant dependence of M_z and the line shape upon H_1 .

To summarize the aluminum measurements, all observations are in agreement with conclusions based on the Redfield picture of the saturated system.

IV. SUMMARY

We have described a double-magnetic-resonance scheme by means of which it is possible to study conditions of energy transfer within a single spin system when rf energy is poured into the system at a single frequency. The measurements in $\text{CaSO}_4 \cdot 2\text{H}_2\text{O}$ illustrate an application to a system with resolved structure in which one can study the disturbance of population differences between one pair of levels by saturation of another pair. The aluminum measurements demonstrate directly certain features of the saturation behavior of a homogeneously broadened resonance line. They extend somewhat the range of experimental verification of the validity of Redfield's description of a saturated system in terms of a canonical distribution of states with respect to the system Hamiltonian as expressed in a frame rotating at the frequency ω_1 . It should be mentioned that a very direct and elegant experiment demonstrating the validity of Redfield's effective spin temperature concept has very recently been performed by Slichter and Holton.¹⁶

Our particular experimental arrangement is limited to systems in which the resonance line is broad. Interaction between the two oscillators sets a lower limit on the frequency difference $\omega_1 - \omega_2$. The technique may also be useful for certain electron spin systems, although

the experimental problems at microwave frequencies are a bit more difficult to solve.

ACKNOWLEDGMENTS

We wish to thank the Advanced Research Projects Agency for assistance in the final phases of this work, this assistance being provided through the Cornell Materials Science Center.

APPENDIX

It is perhaps worthwhile noting that Eq. (4), obtained from the Bloch equations modified by the insertion of T_{2e} , gives a behavior of M_z qualitatively similar to the Redfield expression if one makes the assumption that $T_{2e} = T_2(1+S)$. With that assumption, Eq. (4) becomes

$$M_z = M_0 \frac{1/(1+S) + (\omega_1 - \omega_0)^2 T_2^2}{1 + (\omega_1 - \omega_0)^2 T_2^2}, \quad (5)$$

and one sees again the weak dependence on H_1 when ω_1 is appreciably off resonance. There are other reasons for the introduction of the semiempirical relation $T_{2e} = T_2(1+S)$. As Redfield points out, one expects T_{2e} to make a transition from a value equal to T_2 at low rf level to an eventual value about equal to T_1 at very large H_1 . But this transition would be expected to occur over a considerable range of H_1 . The particular form of the dependence of T_2 on H_1 is suggested by solving the Bloch equations for χ' after the insertion of T_{2e} . The nonsaturation of χ' (until H_1 becomes of the order of the local fields) derived by Redfield follows directly from this solution if one assumes $T_{2e} = T_2(1+S)$. The relation is

$$\chi' = \frac{1}{2} \chi_0 \omega_0 T_2^2 \frac{(\omega_0 - \omega_1)(1+S)}{[1 + (\omega_0 - \omega_1)^2 T_2^2](1+S)}. \quad (6)$$

With the same assumption about T_{2e} , the steady-state solution for the imaginary part of the rf susceptibility is

$$\chi'' = \frac{1}{2} \chi_0 \omega_0 T_2 \{1/[1 + (\omega_0 - \omega_1)^2 T_2^2](1+S)\}, \quad (7)$$

and we see that the lack of saturation broadening in χ'' , which comes from the Redfield theory, also appears. Obviously, none of (5), (6), or (7) would be expected to obtain at very high H_1 , since T_{2e} will eventually level off in some fashion to a value approximately equal to T_1 . In solids, the Bloch equations are, of course, useful primarily to provide semiquantitative guides to the understanding of various phenomena. Introduction of the variable T_{2e} extends their usefulness somewhat.

¹⁶ C. P. Slichter and W. C. Holton, Phys. Rev. **122**, 1701 (1961).